

## Numerical modeling of EM fields over local anomalies with a vertical axis of symmetry

Michael S. Zhdanov, Vjacheslav V. Spichak and Leonid Yu. Zaslavsky

*Institute of Terrestrial Magnetism, Ionosphere, and Radio Wave Propagation (IZMIRAN), U.S.S.R. Academy of Sciences, 142092  
Troitsk, Moscow Region (U.S.S.R.)*

(Received August 20, 1987; revision accepted November 27, 1988)

Zhdanov, M.S., Spichak, V.V. and Zaslavsky, L.Yu., 1990. Numerical modeling of EM fields over local anomalies with a vertical axis of symmetry. *Phys. Earth Planet. Inter.*, 60: 53-61.

A method for numerical modeling of quasi-stationary electromagnetic fields in axially symmetric media is proposed. It is based on the direct finite-element method and the use of special basis functions. Assuming cylindrical coordinates  $r$ ,  $\phi$ ,  $z$ , the three-dimensional solution is presented as a superposition of fields with the azimuthal dependence  $\exp(in\phi)$ . For each case this results in a system of two equations of elliptical type in two scalar functions in the  $(r, z)$  plane.

The discretization leads to the conservative nine-points difference scheme. The system of linear equations is solved by means of the LU-decomposition technique, the band structure of the matrix being taken into account.

The program is tested using analytical results (DC asymptote) for a near-surface inhomogeneity. Comparison also is made with 2D results ( $H$ -polarization) for the model of a local well conducting inclusion in a three-layered Earth.

### 1. Introduction

Analysis and interpretation of transient electromagnetic field anomalies in the Earth, investigation of the resolution of soundings as well as a number of other problems encountered today in geoelectrics (Berdichevsky and Zhdanov, 1984) require computer-assisted calculation of many different models. These problems can be solved in principle by using existing methods of numerical modeling of electromagnetic fields in media that include arbitrary three-dimensional inhomogeneities (e.g., review paper by Hohmann (1983)). However, this objective can be achieved with reduced computer resources if we restrict ourselves to models of a specific type of symmetry. In particular, axially symmetric three-dimensional models reduce the vector problem to a series of independent problems in a plane for two scalar functions (Zakharov, 1978). In this case, the reduction to a discrete system may be accomplished either by the

integral equation method (Zakharov, 1978; Barashkov and Dmitriev, 1982) or by one of the differential equation methods (Zhdanov et al., 1984).

In this work we suggest an algorithm for the numerical modeling of quasi-stationary electromagnetic fields in axially symmetric three-dimensional media. The algorithm relies on finite-element modification of the balance method which has shown good results for the solution of two- and three-dimensional problems (Zhdanov et al., 1982; Spichak, 1983).

### 2. Basic equations and boundary conditions

#### 2.1. Problem statement

Consider an electromagnetic field excited by a plane vertically incident wave in a layered medium

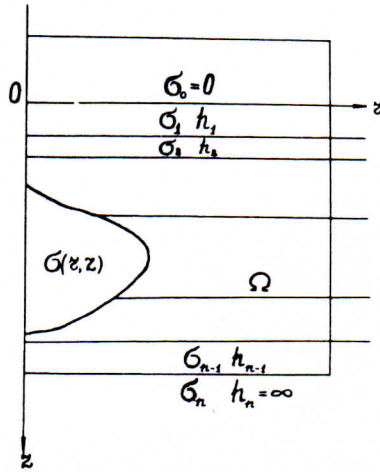


Fig. 1. Model of the geoelectric section (in cylindrical coordinates);  $\Omega$  is the domain of modeling.

that includes a three-dimensional axially symmetric inhomogeneity (Fig. 1). The medium is assumed to be isotropic and non-magnetic. The magnetic permeability in the whole space is taken to be equal to permeability of free space ( $\mu = \mu_0$ ). Displacement currents are neglected, i.e., the field is assumed to be quasi-stationary. The time dependence of the fields is defined by the factor  $\exp(-i\omega t)$ . Maxwell's equations for quasi-stationary field harmonics then have the form

$$\begin{aligned} \text{curl } \mathbf{H} &= \sigma \mathbf{E} \\ \text{curl } \mathbf{E} &= i\omega\mu_0 \mathbf{H} \end{aligned} \quad (1)$$

We will introduce a cylindrical coordinate system  $(r, \phi, z)$  whose axis coincides with the axis of symmetry of the inhomogeneity and is positive vertically downwards (Fig. 1).

## 2.2. Differential equations for azimuthal components of harmonics

Following Zakharov (1978), we will represent the components of the vectors  $\mathbf{E}$ ,  $\mathbf{H}$  as Fourier series

$$\begin{aligned} E_{r,\phi,z} &= \sum_{n=-\infty}^{+\infty} E_{r,\phi,z}^{(n)} \exp(in\phi) \\ H_{r,\phi,z} &= \sum_{n=-\infty}^{+\infty} H_{r,\phi,z}^{(n)} \exp(in\phi) \end{aligned} \quad (2)$$

Substituting these expansions into Maxwell's equations we derive the following system of equations for harmonics

$$\frac{in}{r} H_z^{(n)} - \frac{\partial H_\phi^{(n)}}{\partial z} = \sigma E_r^{(n)} \quad (3)$$

$$\frac{\partial H_r^{(n)}}{\partial z} - \frac{\partial H_z^{(n)}}{\partial r} = \sigma E_\phi^{(n)} \quad (4)$$

$$\frac{1}{r} H_\phi^{(n)} + \frac{\partial H_\phi^{(n)}}{\partial r} - \frac{in}{r} H_r^{(n)} = \sigma E_z^{(n)} \quad (5)$$

$$\frac{in}{r} E_z^{(n)} - \frac{\partial E_\phi^{(n)}}{\partial z} = i\omega\mu_0 H_r^{(n)} \quad (6)$$

$$\frac{\partial E_r^{(n)}}{\partial z} - \frac{\partial E_z^{(n)}}{\partial r} = i\omega\mu_0 H_\phi^{(n)} \quad (7)$$

$$\frac{1}{r} E_\phi^{(n)} + \frac{\partial E_\phi^{(n)}}{\partial r} - \frac{in}{r} E_r^{(n)} = i\omega\mu_0 H_z^{(n)} \quad (8)$$

Let  $u = E_\phi^{(n)}$  and  $v = H_\phi^{(n)}$ . Using eqns. (3), (8) and (5), (6) we express the components  $E_r^{(n)}$ ,  $H_z^{(n)}$  and  $E_z^{(n)}$ ,  $H_r^{(n)}$  in terms of  $u$  and  $v$

$$\begin{aligned} E_r^{(n)} &= in\hat{D}_r u - i\omega\mu_0 r \hat{D}_z v \\ E_z^{(n)} &= in\hat{D}_z u + i\omega\mu_0 r \hat{D}_r v \\ H_r^{(n)} &= -\sigma r \hat{D}_z u + in\hat{D}_r v \\ H_z^{(n)} &= \sigma r \hat{D}_r u + in\hat{D}_z v \end{aligned} \quad (9)$$

where

$$\hat{D}_r = \frac{r}{\alpha} \left( \frac{\partial}{\partial r} + \frac{1}{r} \right) \quad \hat{D}_z = \frac{r}{\alpha} \frac{\partial}{\partial z}$$

are the components of the vector differential operator

$$\hat{\mathbf{D}} = \begin{bmatrix} \hat{D}_r \\ \hat{D}_z \end{bmatrix}$$

and  $\alpha = i\omega\mu_0 \sigma r^2 - n^2$ .

Substituting these expressions into (4) and (7) gives equations in  $u$  and  $v$

$$\begin{aligned} \text{div}_2(\sigma r \hat{D}_z u) + \sigma u - in \cdot \text{curl}_2(\hat{D}_z v) &= 0 \\ \text{div}_2(i\omega\mu_0 r \hat{D}_r v) + i\omega\mu_0 v - in \text{curl}_2(\hat{D}_r u) &= 0 \end{aligned} \quad (10)$$

where

$$\begin{aligned} \text{div}_2 &= \mathbf{e}_r \frac{\partial}{\partial r} + \mathbf{e}_z \frac{\partial}{\partial z} \\ \text{curl}_2 &= \mathbf{e}_r \frac{\partial}{\partial z} - \mathbf{e}_z \frac{\partial}{\partial r} \end{aligned}$$

where  $e_r$  and  $e_z$  are the unit vectors of the cylindrical coordinate system.

It is evident that when the field is excited by a plane wave it is sufficient to solve the problem for harmonics  $n = \pm 1$  (Barashkov and Dmitriev, 1982). If the normal field is polarized linearly (with the magnetic field in the  $\phi = \pi/2$  azimuth), the harmonics  $n = 1$  and  $n = -1$  are related by

$$\begin{aligned} E_\phi^{(-1)}(r, z) &= -E_\phi^{(1)}(r, z) \\ H_\phi^{(-1)}(r, z) &= H_\phi^{(1)}(r, z) \end{aligned} \quad (11)$$

Hence, to determine the electromagnetic field components within an axially symmetric three-dimensional model, it is sufficient to define the  $u$  and  $v$  functions corresponding to value  $n = 1$  and then to determine the required field by formula (2) with reference to relations (9) and (11).

### 2.3. Boundary conditions

Without loss of generality, the domain of modeling is assumed to be a rectangle  $\Omega$  on the plane  $(r, z)$  whose left-hand side lies on the  $z$  axis, the upper side is in the atmosphere, and the lower side is located in the underlying basement (Fig. 1). On the boundaries of the domain  $\Omega$  the following boundary conditions are specified.

(a) On the upper boundary in the atmosphere (and on the lower boundary if the underlying basement is highly resistive) the first-order asymptotic boundary conditions for an anomalous field

$$\left(1 + r \frac{\partial}{\partial r} + z \frac{\partial}{\partial z}\right)(u - u^n) = 0$$

$$\left(1 + r \frac{\partial}{\partial r} + z \frac{\partial}{\partial z}\right)(v - v^n) = 0$$

are valid, where  $u$  and  $v$  are the azimuthal components of harmonics of the total field, while  $u^n$  and  $v^n$  are those of the normal field. These conditions are readily established from the asymptotic boundary conditions derived by Zhdanov et al. (1982) and Spichak (1985).

(b) At the interface of a highly conducting underlying basement, which can be roughly considered as a perfect conductor, the horizontal

components of the electric field are zero. This leads to the boundary conditions

$$u = 0 \quad \frac{\partial v}{\partial z} = 0$$

(c) On the axis of symmetry, the exact relations

$$\frac{\partial u}{\partial r} = 0 \quad \frac{\partial v}{\partial r} = 0$$

are satisfied.

(d) On the right-hand boundary of the modeling domain, the total field is locally approximated by a plane vertically incident wave. In this case, the boundary conditions are

$$\frac{\partial u}{\partial r} = 0 \quad \frac{\partial v}{\partial r} = 0$$

### 3. Formulation of discrete equations and their numerical solution

To derive discrete equations, we will utilize a direct finite-element method (Norrie and de Vries, 1978). In this case, it is helpful to set up a conservative scheme around a nine-point pattern.

#### 3.1. Discrete equations

Introduce a grid  $\Sigma$  on a plane  $(r, z)$ :  $(r_i, z_j) \in \Sigma$ ,  $1 < i < I$ ,  $1 < j < J$

Unit cells are rectangles  $S_{kl}$  ( $k = 1, 2, \dots, I$ ;  $l = 1, 2, \dots, J$ ) whose vertices are in the middle of the cells of the grid  $\Sigma$  that are adjacent to grid points  $(r_i, z_j)$  (Fig. 2).

Integrating eqns. (10) over an area of the cells  $S_{kl}$  and using the Ostrogradsky-Gauss and Stokes two-dimensional formulae (Berdichevsky and Zhdanov, 1984), we obtain the balance equations

$$\int_{S_{kl}} \sigma r (\hat{\mathbf{D}}\mathbf{u})_v dl + \int_{S_{kl}} \sigma u dS - in \int_{S_{kl}} (\hat{\mathbf{D}}\mathbf{v})_l dl = 0$$

$$\int_{S_{kl}} i\omega\mu_0 r (\hat{\mathbf{D}}\mathbf{v})_v dl + \int_{S_{kl}} i\omega\mu_0 v dS \quad (12)$$

$$- in \int_{S_{kl}} (\hat{\mathbf{D}}\mathbf{u})_l dl = 0$$

where  $S_{kl}$  is the boundary of the cell  $S_{kl}$ ,  $\mathbf{v}$  and  $\mathbf{l}$  are the unit vectors directed along an outward pointing normal and a tangent to the boundary  $S_{kl}$ , respectively; the contour  $S_{kl}$  is traversed counterclockwise.

We will seek  $u$  and  $v$  as an expansion in terms of finite basis functions

$$\begin{aligned} u(r, z) &= \sum_{i=1}^I \sum_{j=1}^J u_{ij} \phi_{ij}(r, z) \\ v(r, z) &= \sum_{i=1}^I \sum_{j=1}^J v_{ij} \phi_{ij}(r, z) \end{aligned} \quad (13)$$

where  $\phi_{ij}(r, z) = 0$ , if  $(r, z) \notin [r_{i-1}, r_{i+1}] \times [z_{j-1}, z_{j+1}]$ .

Substituting eqn. (13) into eqn. (12) we write

$$\begin{aligned} \sum_{i=k-1}^{k+1} \sum_{j=l-1}^{l+1} (A_{kl}^{ij} u_{ij} + B_{kl}^{ij} v_{ij}) &= 0 \\ \sum_{i=k-1}^{k+1} \sum_{j=l-1}^{l+1} (B_{kl}^{ij} u_{ij} + C_{kl}^{ij} v_{ij}) &= 0 \end{aligned} \quad (14)$$

( $k = 1, 2, \dots, I$ ;  $l = 1, 2, \dots, J$ )

where

$$\begin{aligned} A_{kl}^{ij} &= \int_{S_{kl}} \sigma(r, z) r (\hat{\mathbf{D}} \phi_{ij}) \mathbf{v} dl \\ &+ \iint_{S_{kl}} \sigma(r, z) \phi_{ij} dS \end{aligned}$$

$$B_{kl}^{ij} = -in \int_{S_{kl}} (\hat{\mathbf{D}} \phi_{ij}) \mathbf{l} dl$$

$$C_{kl}^{ij} = i\omega\mu_0 \left[ \int_{S_{kl}} r (\hat{\mathbf{D}} \phi_{ij}) \mathbf{v} dl + \iint_{S_{kl}} \phi_{ij} dS \right]$$

Definite integrals entering the formulas for the coefficients  $A_{kl}^{ij}$ ,  $B_{kl}^{ij}$ , and  $C_{kl}^{ij}$  are calculated numerically.

### 3.2. Basis functions

As is known, allowance for the field behaviour contributes to the accuracy of equation approximation. Assuming that in the neighbourhood of each point of the grid, total fields vary linearly in

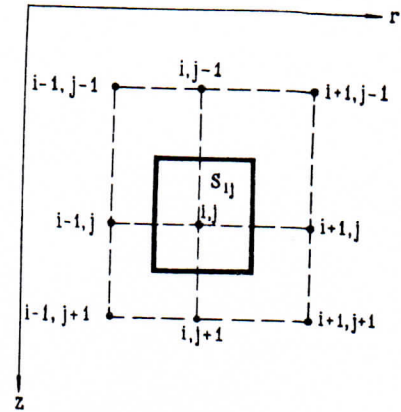


Fig. 2. Unit cell  $S_{ij}$  of the rectangular mesh.

the horizontal and exponentially in the vertical, we can introduce the following basis functions

$$\phi_{ij}(r, z) = \xi_{ij}(r) \eta_{ij}(z) \quad (15)$$

where

$$\xi_i(r) = \begin{cases} 0 & r < r_{i-1} \\ \frac{r - r_{i-1}}{r_i - r_{i-1}} & r_{i-1} \leq r \leq r_i \\ \frac{r_{i+1} - r}{r_{i+1} - r_i} & r_i \leq r \leq r_{i+1} \\ 0 & r_{i+1} \leq r \end{cases}$$

$$\eta_{ij}(r, z) = \begin{cases} 0 & z \leq z_{j-1} \\ \frac{\sinh(k_{ij}^+(z - z_{j-1}))}{\sinh(k_{ij}^+(z_j - z_{j-1}))} & z_{j-1} \leq z \leq z_j \\ \frac{\sinh(k_{ij}^-(z - z_{j+1}))}{\sinh(k_{ij}^-(z_j - z_{j+1}))} & z_j \leq z \leq z_{j+1} \\ 0 & z_{j+1} \leq z \end{cases}$$

where

$$k_{ij}^+ = \sqrt{-i\omega\mu_0\sigma_{ij}^+}, \quad k_{ij}^- = \sqrt{-i\omega\mu_0\sigma_{ij}^-}$$

are the average conductivities in the upper and lower halves of a cell respectively.

Derived basis functions possess fairly good approximation properties. In particular, the normal field calculated for a one-dimensional conducting

medium from a system of eqns. (14) with due account of eqn. (15) coincides with that calculated analytically. It should be noted that if  $k_{ij} \rightarrow 0$ ,  $\eta_{ij}(x)$  reduces to the function  $\xi_i(x)$ .

### 3.3. Numerical solution of discrete equations

The system of linear algebraic equations resulting from discretization is solved by employing the Crout algorithm of expanding a matrix into the product of the upper and lower triangular matrices (Tearson, 1973). Below is a brief outline of the algorithm.

Represent the matrix  $A$  ( $N \times N$ ) of the system in the form

$$A = \begin{bmatrix} d & \omega^T \\ \mathbf{v} & G \end{bmatrix}$$

where  $d$  is a scalar,  $\mathbf{v}$  is a column vector,  $\omega^T$  is a row vector,  $G$  is an  $(N-1)$ th order square matrix. One can see that for  $d \neq 0$ , the following representation

$$A = \begin{bmatrix} d & \mathbf{0}^T \\ \mathbf{v} & I_{N-1} \end{bmatrix} \cdot \begin{bmatrix} 1 & \mathbf{0}^T \\ \mathbf{0} & G' \end{bmatrix} \cdot \begin{bmatrix} 1 & \omega^T/d \\ 0 & I_{N-1} \end{bmatrix}$$

holds, where the  $(N-1)$ th order square matrix  $G'$  is defined by

$$G' = G - \frac{\mathbf{v}\omega^T}{d}$$

$I_{N-1}$  is an  $(N-1)$ th order identity matrix,  $\mathbf{0}$  is a zero column vector. In the next step, the matrix  $G'$  is expanded in the same way, etc. As a result, in  $N$  steps, the initial matrix is expanded into the product of the upper and lower triangular matrices. Upon expansion, the lower and upper triangular system of equations are solved.

The system of linear algebraic equations resulting from discretization has a banded structure (the band width  $M = 4 + 2 \cdot \min(I, J)$ , where  $I$  and  $J$  are the numbers of grid points in the vertical and in the horizontal, respectively). The application of the Crout algorithm to this matrix is distinguished by the following feature. In each step of the algorithm all operations are performed on the matrix elements lying inside a square  $\Lambda(M \times M)$  which slides diagonally downwards (Fig. 3). In doing so, we obtain the relevant column of the

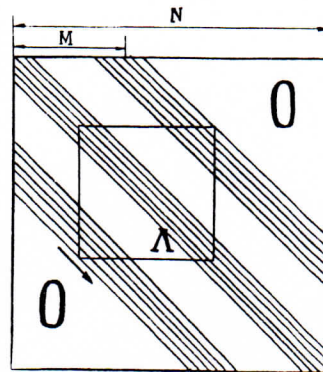


Fig. 3. Structure of the system matrix:  $N$  is the matrix size,  $M$  is the band width.

lower triangular matrix and a row of the upper triangular matrix. This permits matrix expansion by parts, utilizing a disk direct-access file and a small portion of the core memory.

The algorithm has been implemented for complex matrices in real arithmetic.

## 4. Program testing

### 4.1. The FDMS-3D program

The above algorithm has been used to develop a program of numerical modeling of monochromatic electromagnetic fields in the Earth containing an axially symmetric three-dimensional inhomogeneity. The program is written in FORTRAN-IV. It is applicable to computers with a core memory greater than 128 kbytes. Its execution requires also magnetic disk space as large as 500 to 4000 kbytes (depending on the number of grid points).

The FDMS-3D program was employed to calculate the response of a model of a cylindrical insert for which an approximate analytical solution is available in the case of DC-asymptotics (Berdichevsky and Dmitriev, 1976).

### 4.2. Fixed-depth isometric depression (cylindrical insert)

The model is shown in Fig. 4. It consists of a thin layer,  $h_1$  of a constant resistivity  $\rho_1^e$  (integral

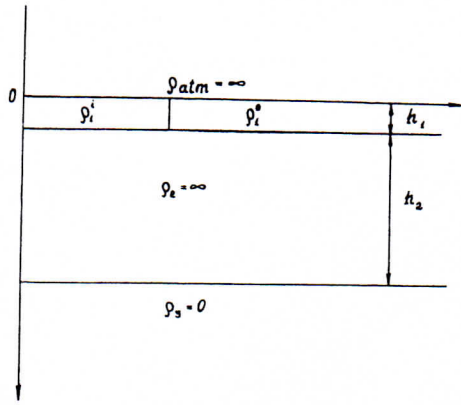


Fig. 4. Model of a cylindrical insert with resistivity  $\rho_1^i$ .

conductivity  $S_1^c$ ), a non-conducting intermediate layer ( $\rho_2 = \infty$ ) of thickness  $h_2$ , and a perfectly conducting underlying basement ( $\rho_3 = 0$ ). The upper layer includes a cylindrical insert of resistivity  $\rho_1^i$  and radius  $a$  which is the same thickness as the upper layer (integral conductivity  $S_1^i$ ).

For DC-asymptotics this model has an analytical solution (Berdichevsky and Dmitriev, 1976) implying that

$$E_\alpha = F_\alpha E_\alpha^n, \quad \alpha = r, \phi \quad (16)$$

where  $E_{r,\phi}$  stands for the components of the total field, while  $E_{r,\phi}^n$  designates the components of the normal field

$$F_r = \begin{cases} 1 - \frac{S_1^i - S_1^c}{S_1^i + S_2^c} & 0 \leq r \leq a \\ 1 + \frac{S_1^i - S_1^c}{S_1^i + S_1^c} \frac{a^2}{r^2} & r \geq a \end{cases}$$

$$F_\phi = \begin{cases} 1 - \frac{S_1^i - S_1^c}{S_1^i + S_2^c} & 0 \leq r \leq a \\ 1 - \frac{S_1^i - S_1^c}{S_1^i + S_1^c} \frac{a^2}{r^2} & r \geq a \end{cases}$$

The value of an anomalous magnetic field for the DC-asymptotics is defined, according to Berdichevsky and Dmitriev (1976), by the asymptotic formula

$$\mathbf{H}^a \mathbf{e}_z = \frac{1}{2} (S_1 \mathbf{E} - S_1^c \mathbf{E}^n) \quad (17)$$

where  $S_1^i = S_1$ , if  $0 \leq r \leq a$  and  $S_1^c = S_1$ , if  $r \geq a$ .

Calculations were made for the following model parameters:  $h_1 = 0.5$  km;  $h_2 = 10$  km;  $a = 5$  km;  $S_1^c = 500$  S;  $S_1^i = 2500$  S;  $\sigma_2 = 10^{-5}$  S m $^{-1}$ ;  $\sigma_3 = 10^5$  S m $^{-1}$ ; at periods  $T = 21, 84$  and  $360$  s.

Figure 5 gives normalized values of the azimuthal component of the electric field for several periods calculated by the FDMS-3D program and defined by asymptotic formula (16) ( $T = \infty$ ).

It is evident from Fig. 5 that at  $T = 84$  s, the  $E_\phi$  plot differs from the asymptotic curve by a maximum 2–3% where the knee on the boundary of the inclusion is smoothed. The curve for  $T = 21$  s differs markedly from the asymptotic curve over the anomaly, which is due to the induction effect. But starting from  $r = 5.5$  km ( $r/a = 1.1$ ) the curves come closer together and differ by not more than 2–4%.

Figure 6 shows values of the quantity  $|H_\phi^a|/|H_{\phi,\text{anal}}^a(0)|$  found by executing the FDMS-

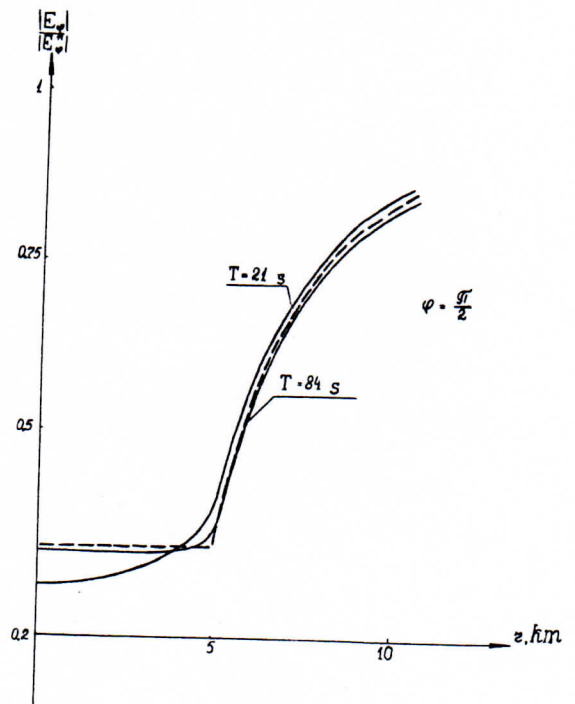


Fig. 5. Normalized  $E_\phi$  values at the Earth's surface within the model of a cylindrical insert, shown in Fig. 4; the solid curves represent the results calculated by the FDMS-3D program, the dashed curve designates the results obtained by the analytical formula.

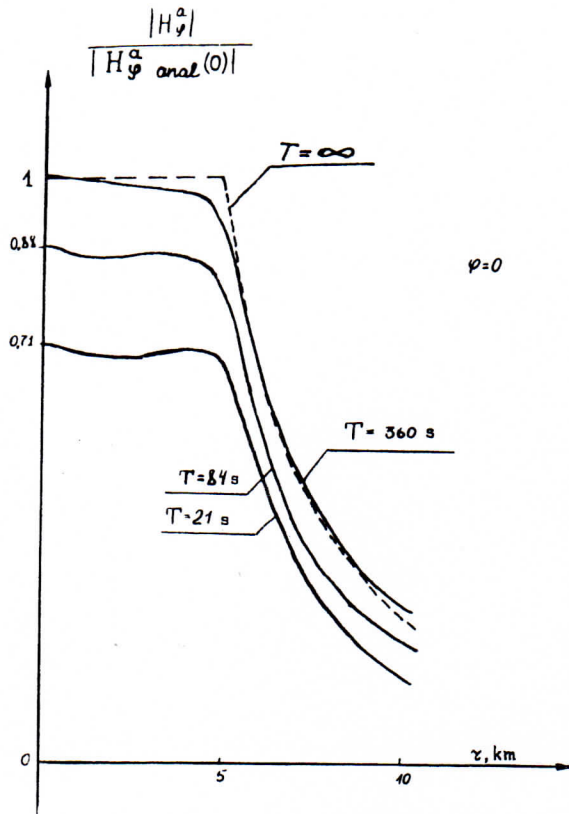


Fig. 6. Normalized values of the anomalous magnetic field at the Earth's surface within the model of a cylindrical insert shown in Fig. 4; the solid curves represent the results calculated by the FDMS-3D program, the dashed curve designates the results obtained by the analytical formula.

3D program for periods 21, 85 and 360 s and the asymptotic formula (17) ( $T = \infty$ ).

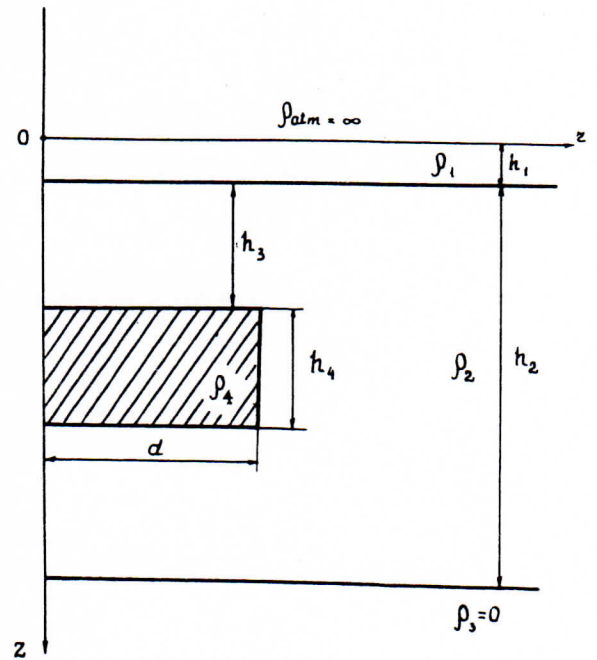
Because of inductive interaction, the  $H_{\phi}$  curve for  $T = 21$  s differs markedly from the asymptotic one (at the center of the anomaly) by 30%. As the period becomes longer, inductive interaction decreases. Thus, the curve for  $T = 84$  s differs from the asymptotic one by 12%, while the curve plotted for  $T = 360$  s follows virtually the asymptotic curve, with the only difference that the former is a smoother version of the latter; the difference is 0.2% at the center of the anomaly, 3% for  $r = 7$  km ( $r/a = 1.4$ ), and 8% on the boundary of the anomaly (for  $r = 5$  km).

It is noteworthy that calculations have been carried out for a relatively small grid  $20 \times 30$ .

4.3. Cylindrical conducting inclusion

Our calculations relate to a model within which a highly conducting layer of resistivity  $\rho_1$  and a poorly conducting layer of resistivity  $\rho_2$  are on a plane surface of a perfect conductor. The  $\rho_2$  layer contains a cylindrical inclusion (Fig. 7). A two-dimensional statement of the problem was considered by Berdichevsky et al. (1982). Calculations were made for the following parameters:  $h_1 = 1$  km,  $\rho_1 = 1 \Omega \text{ m}$ ,  $h_2 = 50$  km,  $\rho_2 = 100 \Omega \text{ m}$ ,  $\rho_3 = 0$ ,  $\rho_4 = 0.1 \Omega \text{ m}$ ,  $h_3 = 5$  km,  $h_4 = 4$  km. Two cases:  $d = 4$  km and  $d = 50$  km, were considered.

With  $d = 4$  km, the conducting layer exerts a strong screening effect on the thin well conducting inclusion. At the surface of the Earth the anomaly



- $\rho_1 = 1 \text{ Ohm}\cdot\text{m}, \quad h_1 = 1 \text{ km}$
- $\rho_2 = 100 \text{ Ohm}\cdot\text{m}, \quad h_2 = 50 \text{ km}$
- $\rho_3 = 0, \quad h_3 = 5 \text{ km}$
- $\rho_4 = 0,1 \text{ Ohm}\cdot\text{m} \quad h_4 = 4 \text{ km}$
- a)  $d = 4 \text{ km}$
- b)  $d = 50 \text{ km}$

Fig. 7. The testing model from Berdichevsky and Dmitriev (1976).

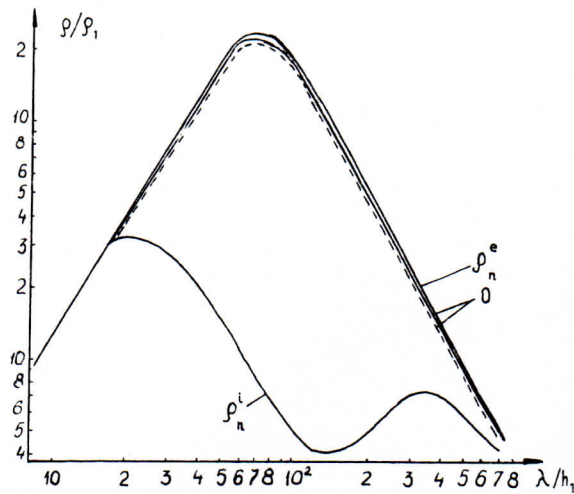


Fig. 8. Apparent resistivity  $\rho_{xy}/\rho_1$  for the model shown in Fig. 7, with  $d = 4$  km (solid lines are 3D results; dashed line is 2D results,  $H$ -polarization;  $\rho_n^e$ ,  $\rho_n^i$ , apparent resistivities for 1D-normal section without insertion and with insertion with  $d = \infty$ , respectively).

is hardly detectable (Fig. 8). In this case, the three-dimensional situation is approximated fairly well by a two-dimensional model of  $H$ -polarization.

As  $d$  increases, along with conductive redistribution of the current, magnetic and inductive effects of the current flowing into the inclusion become important. Figures 9 and 10 show plots of apparent resistivities for  $d = 50$  km along two orthogonal azimuths  $\phi = 0$  and  $\phi = \pi/2$  (the normal electric field is linearly polarized at azimuth  $\phi = 0$ ). A comparison of these findings with the curves for  $E$ - and  $H$ -polarization (Berdichevsky et al., 1982) suggest that for  $d = 50$  km the behavior of the  $\rho_{xy}$  curves along azimuths  $\phi = 0, \pi/2$  resembles qualitatively that of apparent resistivity curves for  $H$ - and  $E$ -polarizations, respectively.

## 5. Conclusions

The results of test calculations and practical experience with the FDMS-3D program demonstrate that the direct finite-element method with special basis functions is an effective means of numerical modeling of quasi-stationary electromagnetic fields in three-dimensional media ex-

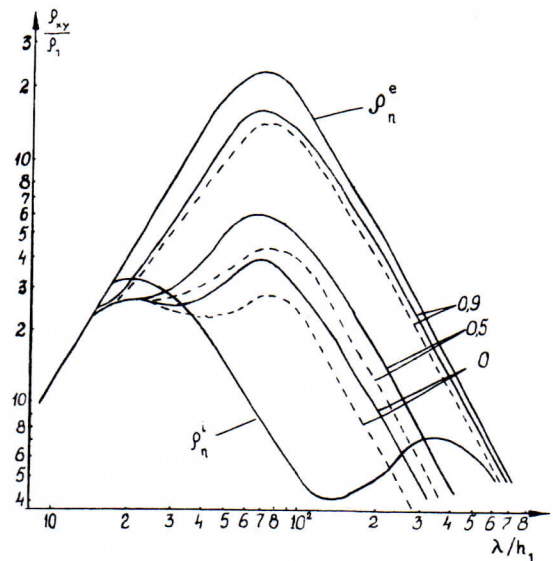


Fig. 9. Apparent resistivity  $\rho_{xy}/\rho_1$  for the model, shown in Fig. 7, with  $d = 50$  km ( $\phi = 0$ ;  $r/d = 0; 0.5; 0.9$ ).

hibiting an axial symmetry. The FDMS-3D program does not require appreciable computer resources and applies equally to purely methodical calculations and to the solution of a fairly wide range of practical geoelectrical problems.

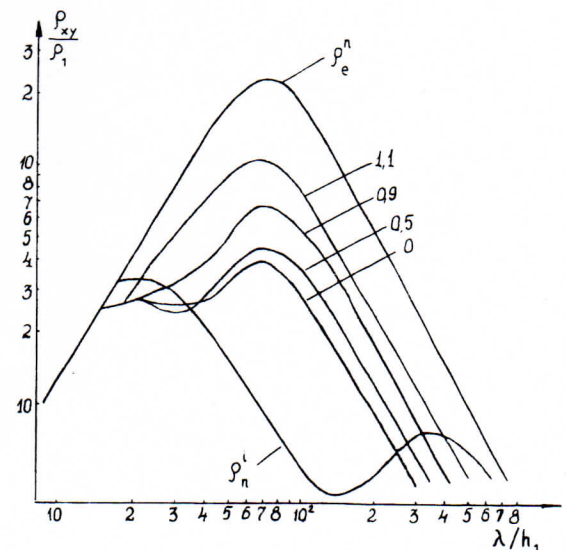


Fig. 10. Apparent resistivity  $\rho_{xy}/\rho_1$  for the model, shown in Fig. 7, with  $d = 50$  km ( $\phi = \pi/2$ ;  $r/d = 0; 0.5; 0.9; 1.1$ ).



### Acknowledgments

We wish to thank Dr. I.S. Barashkov of Moscow State University, who kindly gave us the results of two-dimensional calculations. Authors are also grateful to the referees and editor for their valuable suggestions and corrections in the manuscript.

### References

- Barashkov, I.S. and Dmitriev, V.I., 1982. Method of two-dimensional integral equations for calculating magnetotelluric fields in a layered medium containing an axially symmetric inhomogeneity. In: *Vych. metody i programmirovaniye*. 36. Moscow State University, Moscow, pp. 14-27 (in Russian).
- Berdichevsky, M.N. and Dmitriev, V.I., 1976. Basic principles of interpretation of magnetotelluric sounding curves. In: *Geoelectrical and Geothermal Studies*. Academia, Kiado, Budapest, pp. 165-221.
- Berdichevsky, M.N. and Zhdanov, M.S., 1984. *Advanced Theory of Deep Geomagnetic Sounding*. Elsevier, Amsterdam, 408 pp.
- Berdichevsky, M.N., Dmitriev, V.I., Barashkov, I.S., Mershchikova, N.A. and Kobsova, V.M., 1982. Magnetotelluric sounding of conducting zones in the Earth's crust and upper mantle. *Izv. AN SSSR, ser. Fizika zemly*, 7: 55-68 (in Russian).
- Hohmann, G.W., 1983. Three-dimensional EM modelling. *Geophysical Surveys*, 6: 27-54.
- Norrie, D.H. and de Vries, G., 1978. *An Introduction to Finite-Element Analysis*. Academic Press, New York, 304 pp.
- Spichak, V.V., 1983. Mathematical modeling of electromagnetic fields in three-dimensional inhomogeneous media. Ph.D. thesis. IZMIRAN, Moscow, 215 pp. (in Russian).
- Spichak, V.V., 1985. Differential boundary conditions for electric and magnetic fields in unbounded conductive medium. In: *Elektromagnitnye zondirovaniya Zemli*. IZMIRAN, Moscow, pp. 13-33 (in Russian).
- Tewarson R.P., 1973. *Sparse Matrices*. Academic Press, New York, 189 pp.
- Zakharov, E.V., 1978. Method used to solve boundary electrodynamic problems for axially symmetric inhomogeneous media. In: *Vychislitelnye metody i programmirovaniye*. Moscow State University: 28, pp. 232-238 (in Russian).
- Zhdanov, M.S., Golubev, N.G., Spichak, V.V. and Varentsov, Iv. M., 1982. The construction of effective methods for electromagnetic modelling. *Geophys. J.R. Astron. Soc.*, 68 (3): 589-607.
- Zhdanov, M.S., Spichak V.V. and Zaslavsky L. Yu., 1984. Algorithm of finite-difference modeling of harmonic electromagnetic fields in axially symmetric three-dimensional media. *Elektromagnitnye zondirovaniya*. IZMIRAN, Moscow, p. 19 (in Russian).

$\frac{\delta}{h_1}$   
shown in

3D pro-  
ut 3-  
thouical  
ly wide

$\frac{7\delta}{\lambda/h_1}$   
, shown in  
(1.1).